HYDROSOL OF C$_{70}$ FULLERENE: SYNTHESIS AND STABILITY IN ELECTROLYTIC SOLUTIONS

M. O. Marfunin,[a] V. K. Klochkov,[b] P. M. Radionov,[a] N. O. Mchedlov-Petrossyan[a]

[a] *V. N. Karazin Kharkiv National University, 4 Svoboda sq., Kharkiv, 61022, Ukraine*
[b] *Institute for Scintillation Materials NAS of Ukraine, 61001 Kharkiv, Ukraine*
e-mail: mchedlov@karazin.ua

This article is devoted to the synthesis and characterization of the C$_{70}$ hydrosol of the son/nC$_{70}$ type and to its coagulation by sodium chloride and cetyltrimethylammonium bromide (CTAB). At C$_{70}$ concentration of 3.3×10^{-6} M, the electrokinetic potential is $\zeta = -40 \pm 4$ mV, the particle size expressed as Zeta-average is 97 ± 3 nm; at higher C$_{70}$ concentrations, 1.7×10^{-5} and 6.9×10^{-5} M, the size stays the same: 99 – 100 nm. The critical concentration of coagulation (CCC) values were determined using the diameter increasing rate (DIR) on NaCl concentration. The CCCs are concentration-dependent: 250, 145, and 130 mM at C$_{70}$ concentrations 3.3×10^{-6}, 1.7×10^{-5}, and 6.9×10^{-5} M, respectively. The CCC for the CTAB surfactant is much lower, about 5×10^{-3} mM. At 0.02 mM CTAB, however, the overcharging up to $\zeta = +40$ mV and stabilization of the colloidal particles take place. Interpretation of the hydrosol coagulation by NaCl using the Derjaguin–Landau–Verwey–Overbeek theory makes it possible to determine the Hamaker constant of the C$_{70}$–C$_{70}$ interaction in vacuum, if only electrostatic repulsion and molecular attraction are taking into account: $A_{FF} \approx 7 \times 10^{-20}$ J. On the other hand, if we use the value $A_{FF} = (16.0\text{–}16.6) \times 10^{-20}$ J, obtained earlier in the study of organosols, then the data for hydrosols can be explained only by the introduction of an additional type of interactions. Following the terms of Churaev and Derjaguin, one should take into account the structural contribution to the interaction energy, which stabilizes the hydrosol.

Keywords: fullerene C$_{70}$ hydrosol, electrokinetic potential, sodium chloride, cetyltrimethylammonium bromide, critical concentration of coagulation, Derjaguin – Landau – Verwey – Overbeek theory, Hamaker diagram, fullerene–fullerene Hamaker constant, structural contribution to the inter-particle interaction.

INTRODUCTION. The chemistry of fullerene solutions, including colloidal ones, is still one of the most interesting areas of nanoscience. Recent reviews give some idea of the current state of affairs in this area [1–3]. An important issue is the nature of aqueous suspensions and hydrosols of fullerenes [2]; the results of new detailed studies of these systems were published this year [4–6]. The last work [6] develops a previously published technique of preparation of the C$_{60}$ hydrosol from the fullerene anion radical [7]. Another group of authors [8] published a molecular dynamics simulation study to understand the stabilization of fullerenes in water; the discussion was based on the idea of important role of the oxidized species C$_{60}$O, which was previously put forward by the Ausman's group [9].

During a study of C$_{70}$ organosols in acetonitrile-based solvents and some other systems [10], as well as analogous dispersions of C$_{60}$ [11, 12], we estimated the Hamaker constant, A_{FF}, of fullerene-fullerene interactions basing on the Derjaguin–Landau–Verwey–Overbeek (DLVO) theory. There are, however, two explanations of the data [10]. First one is based on averaging-out all the estimates obtained with different electrolytes. The average A_{FF} value is close to that estimated in aqueous systems [13–15], but the scatter is substantial. Alternatively, utilization of only several selected systems results in a substantially higher A_{FF} [10]. If the last value is accepted, the presence of a strong stabilizing factor in hydrosols should be presumed.

This paper is aimed to characterize the stability of the C$_{70}$ hydrosol of the so-called son/nC$_{70}$ type prepared by a somewhat modified procedure. Earlier Aich et al. [16, 17] studied in detail this hydrosol as well as those

formed by C$_{60}$, C$_{76}$, and C$_{84}$. Values of the critical concentrations of coagulation of fullerene hydrosols and suspensions by electrolytes published in the literature were gathered in a review paper [2].

EXPERIMENT AND DISCUSSION OF THE RESULTS. Preparation of the C$_{70}$ hydrosol. The first stage consisted in preparing a solution of fullerene in benzene. It is importantly to note that the water content in benzene should not exceed 0.01%. A weight amount of C$_{70}$ (NeoTechProduct, >99%) was placed into benzene without intensive mixing; the final concentration was 5×10^{-4} M. The solution was stored for two weeks, stirring slowly every 3–5 days, and then filtered through a 0.22 µm membrane filter. The second stage was aimed to transfer the fullerene from benzene to water. In a 500 ml beaker, 400 ml of deionized water (conductivity ≤ 1.0 µS) was added and 30 ml of a C$_{70}$ benzene solution (2.5×10^{-4} M) was added. The titanium tip of an ultrasonic disperser (22 kHz, 400–600 W) is immersed in the solution. Sonication was performed at reduced pressure of 100 mm. Hg. First, a white emulsion was formed. Then, the solution becomes transparent with brown tint. The solution thus obtained was centrifuged for 15–20 min at 7000–8000 rpm in order to remove the titanium particles and the coarse fraction of C$_{70}$ particles. The supernatant part of the solution is placed in a round-bottomed flask of a rotary evaporator and evaporated at a bath temperature of 65 ºC to 12 – 15 ml. Then the solution is filtered through membrane filters with pore diameters of 0.45 and 0.22µm. The result is a clear dark brown solution containing $(6–8) \times 10^{-4}$ M C$_{70}$.

Determination of the fullerene concentration and molar absorptivity in water. 2 ml of C$_{70}$ aqueous solution are placed in a 10 ml eva-

porating flask and evaporated to dryness on a rotary evaporator. Then, 2 ml of a mixture of water/acetone in a ratio of 1: 1 are poured into the flask and evaporated to dryness. Then 2 ml of acetone is poured into the flask twice and each time is evaporated to dryness. After drying and removing traces of acetone, 2 ml of benzene are placed in the flask and left to dissolve completely. The concentration of the fullerene in the hydrosol, 4.30×10^{-4} M, was estimated using the molar absorptivity of C_{70} in benzene, 44.7×10^3 $M^{-1}cm^{-1}$, at 382.1 nm. {The molar absorptivity in benzene was estimated by 100-fold dilution by highly purified toluene and using the molar absorptivity of C_{70} in toluene used previously [10]}. Then, the molar absorptivity of C_{70} in the hydrosol at 385.7 nm was estimated as 48.0×10^3 $M^{-1}cm^{-1}$. The absorption spectra are presented in Figure 1.
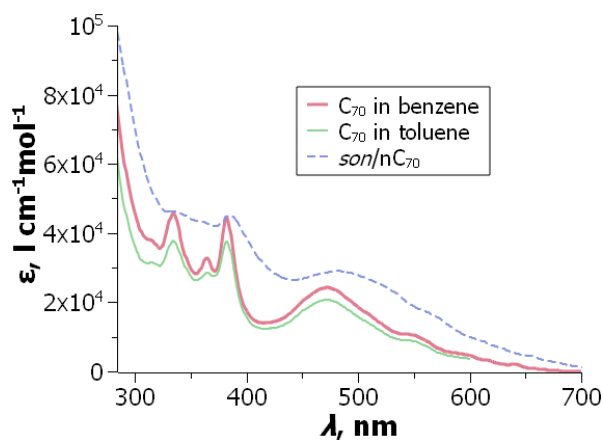

Figure 1 – UV/visible absorption spectra of C_{70} in different media.

This spectrum of the hydrosol is very similar to those reported by Aich et al. [16, 17] and Mikheev et al. [18].

Other chemicals. To determine the hydrosols CCC, the solutions of NaCl (analytical grade) and cetriltrimethylammonium bro-

mide (CTAB, 99 %, Sigma-Aldrich) were used. These solutions were prepared by dissolving of required salt amount in distillate water.

Preparation of the working solutions. The required amount of electrolyte solution was added to the flask, then distillate water. After mixing, an aliquot of the C_{70} stock solution was added to the flask and the solution was stirred again.

Apparatus. UV/visible spectra were run with a Hitachi U-2000 spectrophotometer against solvent blanks. Particle size distribution was obtained using dynamic light scattering via Zetasizer Nano ZS Malvern Instruments, scattering angle 173°; each measurement was made by 12 runs and reproduced at least three times. The values of the ζ-potentials were determined using the Zetasizer Nano ZS Malvern Instruments, scattering angle 12.8°; each measurement was performed by 3–5 runs. The spectral and DLS measurements were made at 25.0 ± 0.5 °C.

Characterization of the hydrosols. Particle size distribution at different fullerene concentrations is presented in Figure 2.
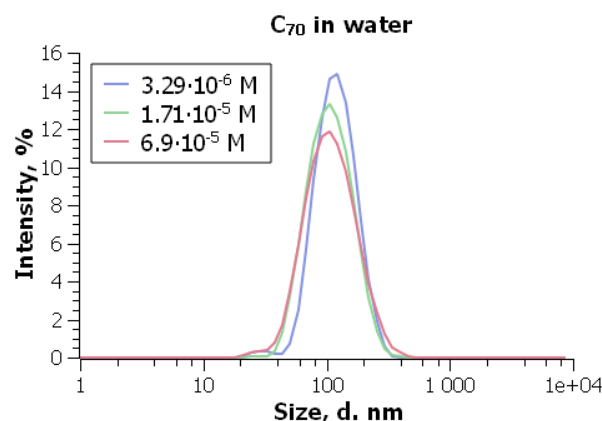

Figure 2 – Particle size distribution of the son/nC_{70} hydrosol at various dilutions of the initial sol.

Main experiments were processed with the concentration of 3.29×10^{-6} M C$_{70}$. The particles are negatively charged, $\varsigma = -40 \pm 4$ mV. The Z-average value is $d = 97 \pm 3$ nm (by number 51 nm; by volume 60; by intensity 110; PDI = 0.18). For C$_{70}$ concentration of 1.71×10^{-5} M, Z-average is 99 nm; the size by number, volume, and intensity is 51; 63; and 114 nm, and PDI = 0.18. For 6.91×10^{-5} M C$_{70}$, the corresponding values are 100 nm; 51; 59; and 120 nm, PDI = 0.22. All the values of the zeta-potential presented here are calculated using the Ohshima equation [19, 20]; in salt-free water, this corresponds to the Onsager–Hückel equation. Note, that other authors [15, 16, 18, 21] use the Smoluchowsky equation.

Aich et al. report the hydrodynamic diameter of 92 ± 14 nm and $\varsigma = -39 \pm 4$ mV [15], Mikheev et al. [18] report $d = 175 \pm 5$ nm (PDI = 0.11 ± 0.02), $\varsigma = -34.4 \pm 0.7$ mV (measurements at 6.2×10^{-5} M C$_{70}$).

Coagulation by sodium chloride. The critical coagulation concentration was determined using the dependence of the diameter increasing rate (DIR) on NaCl concentration (Figure 3), which is in fact a sort of the Fuchs approach [10–15, 17].
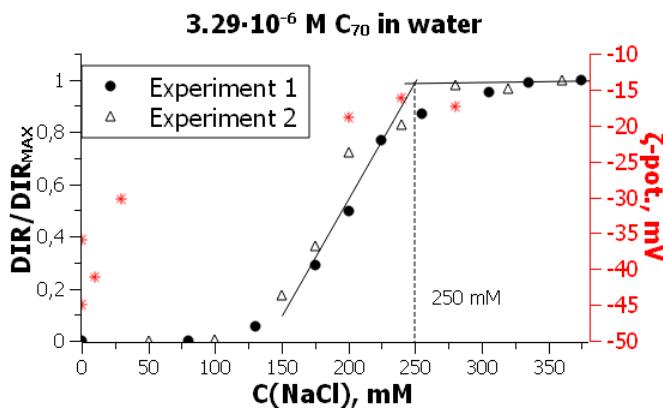

Figure 3 – Determination of the critical coagulation concentration of the C$_{70}$ hydrosol by NaCl: the results of two independent experiments; asterisks indicate the ς values.

The CCC value at 3.3×10^{-6} M C$_{70}$ is 250 mM NaCl. Increasing in the fullerene concentration up to 1.71×10^{-5} M decreases the CCC value down to 145 mM. This is in line with the results obtained with C$_{60}$ hydrosols [2]. Further rise of C$_{70}$ concentration to 6.91×10^{-5} M also decreases the CCC to 130 mM. However, the system is unstable under such conditions, and the coagulation occurs in spurts. Note, that at 1×10^{-4} M of C$_{60}$ hydrosol CCC = 85 mM NaCl (determined by visual titration) [22]. Aich et al. [17] reported a CCC value of 150 mM at 7.9×10^{-7} M C$_{70}$ (the fullerene concentration was calculated using the information on the experimental details kindly sent to us by Dr. Aich).

Interaction of the C$_{70}$ hydrosol particles with CTAB. Small concentrations of CTAB cause charge neutralization of the particles and coagulation of the hydrosol; the size jump approximately corresponds to the isoionic state (Figure 4). The CCC value is about 0.005 mM CTAB. In contrast, further increase in CTAB concentration results in overcharging and
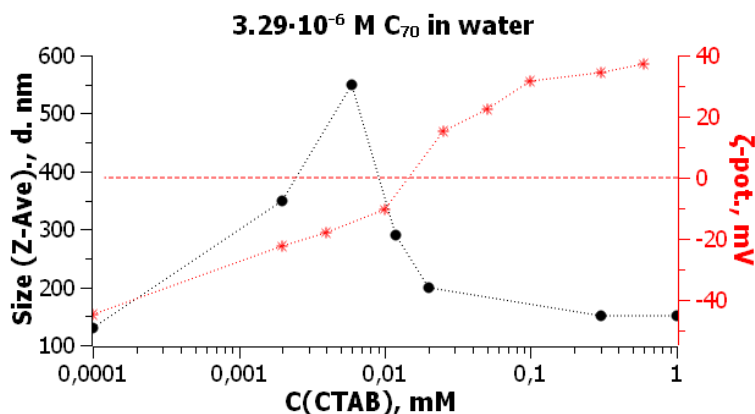
Figure 4 – Size and zeta-potential dependence of the C_{70} colloid in CTAB solutions; asterisks indicate the ς values.

thus stabilization of the sol. This phenomenon is typical for colloidal systems, e.g., for the SiO_2/CTAB [23]. Whereas the coagulation within the range of micromolar CTAB concentrations is obviously caused by adsorption and hence charges neutralization of colloidal particles, the stabilization via particles overcharging is probably a result of surfactant bilayer formation [22, 24].

Interpretation of the CCC(NaCl) value. Despite some differences of the CCCs determined at various C_{70} concentrations and by different authors, these values as well as those for C_{60} hydrosol [2, 13-15, 17, 18, 21, 22], are two-three orders of magnitude higher as compared with the values in organic solvents [10–12]. In both cases, attempts were made to estimate the fullerene–fullerene Hamaker constant, A_{FF}, which characterizes the C_{70}–C_{70} interaction in vacuum, selecting in one way or another a value consistent with a given coagulation threshold. For example, an equation derived by Dukhin et al. [25] can be used, Eq. 1.

$$U = U_{el} + U_{attr} = 64\pi\varepsilon_r\varepsilon_0\left(\frac{RT}{F}\right)^2\text{tgh}^2\left(\frac{\Psi_d F}{4RT}\right)\frac{r\exp(-\kappa h)}{s} - \frac{A^*_{FSF}}{6}\left[\frac{2}{s^2-4}+\frac{2}{s^2}+\ln\frac{s^2-4}{s^2}\right] \quad (1)$$

Here, h is the distance between the centers of the particles, $s = 2 + h/r$, Ψ_d is the electrical surface potential of the colloidal particles, $\varepsilon_0 = 8.854\times 10^{-12}$ F m^{-1}, κ is the reciprocal Debye length, R, T, F have their usual meanings. The measured values of ς can be used for low and medium charged interfaces instead of Ψ_d, in accord to the accepted viewpoint. The A^*_{FSF} value characterizes the fullerene – solvent – fullerene interaction in solution and is

connected with the A_{FF} and A_{SS} values, which characterize the fullerene–fullerene and solvent–solvent interactions in vacuum, respectively, through Eq. 2.

$$A^*_{FSF} = (A_{FF}^{1/2} - A_{SS}^{1/2})^2. \quad (2)$$

Different dependences of U on h can be constructed using various A^*_{FSF} values, and those which meet the coagulation conditions should be selected. Accordingly, the A_{FF} can

be estimated using Eq. 2. In our recent work, in this way we estimated the A^*_{FSF} and A_{FF} values for C$_{70}$ in acetonitrile and methanol (with 10 vol. % toluene) [10]. Using the data for a set of electrolytes, we obtained the A_{FF} values within a wide range of $(5.8 - 16.6) \times 10^{-20}$ J [10]; similar A_{FF} were estimated for C$_{60}$ in acetoni-trile and methanol [11, 12].

At the same time, Elimelech and his co-workers obtained the value $A_{FF} = 7.5 \times 10^{-20}$ J for C$_{60}$ hydrosols prepared by different procedures [13, 15]. Aich et al. [17] used this value for successful explanation of the coagulation of aqueous suspensions of C$_{60}$, C$_{70}$, C$_{76}$, and C$_{84}$. Therefore, the data obtained with organosols can be considered as an approximate estimate, with the value 7.5×10^{-20} J falling within this range.

However, an alternative explanation can be proposed. A careful consideration of the data for organosols demonstrates an expressed tendency to overcharging of the negatively charged colloidal particles of the fullerenes by the metal cations. This most likely leads to hetero- and mutual coagulation, and the simple interpretation of the CCCs using Eq. 1 becomes impossible. Therefore, we selected the data for two electrolytes as coagulators in organic solvents. They are as follows: tetra-*n*-butylammonim perchlorate, chosen because of no signs of overcharging, and calcium perchlorate, which exhibits a second CCC value for completely overcharged C$_{70}$ aggregates [10]. This allows estimating the A_{FF} value $(16.0 - 16.6) \times 10^{-20}$ J [10], which is substantially higher as compared with the "aqueous" value, $A_{FF} = 7.5 \times 10^{-20}$ J. This, in turn, allows suspecting the presence of an additional stabilizing factor in the case of the hydrosols [10].

In Figure 5, series of Hamaker diagrams are presented for ionic strength of 250 mM and $\varsigma = -17$ mV, i.e., under conditions of rapid coagulation by NaCl (see above), and different A^*_{FSF} values; A_{SS} for water is 3.86×10^{-20} J.
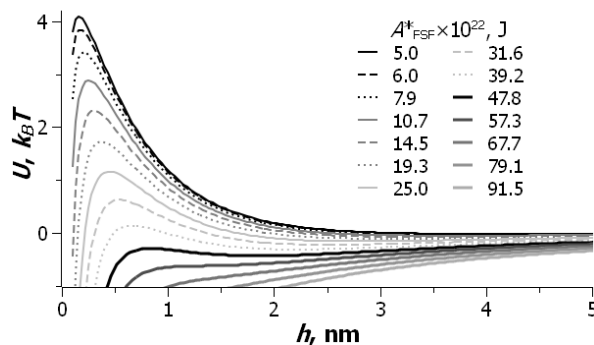

Figure 5 – Hamaker diagrams for the C$_{70}$ hydrosol for 250 mM NaCl.

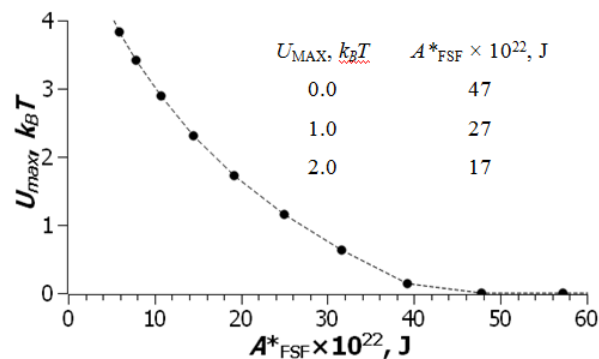In Figure 6, the U_{max} values in $k_B T$ units are plotted against the A^*_{FSF} values.

Figure 6 – Potential barrier height as a function of the Hamaker constant.

If the values of the potential barrier $U_{max} = (0 - 1) k_B T$ are accepted as the margin of the stability, then $A_{FF} = (7.0 \text{ to } 6.2) \times 10^{-20}$ J (Table 1). Average value is 6.6×10^{-20} J; for $U_{max} = 0$, $A_{FF} = 7.0 \times 10^{-20}$ J.

Table 1

Calculated values of the Hamaker constant.

U_{max}, $k_B T$	A^*_{FSF}, 10^{-20} J	A_{FF}, 10^{-20} J
0.00	0.47	7.02
1.00	0.27	6.17
2.00	0.17	5.65
Mean	0.30	6.3

These estimates are in line with the above mentioned publications [13, 15]. On the other hand, if we use the "refined" data obtained from the examination of organosols,

A_{FF} = (16.0 to 16.6)$\times 10^{-20}$ J, then the picture changes radically. In Figure 7, the Hamaker diagrams are constructed with these values. For ionic strength of 100 mM, ς = –22 mV and the DIR value is low but not zero (heavy curve). Here, as well as for higher NaCl concentrations, the system would have to be completely unstable, while experimentally the slow coagulation is observed (Figure 3). At 30 mM NaCl, where the system is quite stable (ς = –30 mV, DIR approaches zero), the barrier height is about 0.5 $k_B T$ (light curves, built for several A_{FF} values from 16.0×10^{-20} J to 16.6×10^{-20} J). Thus, here the rapid coagulation can be expected, which is, however, not the case (Figure 3).
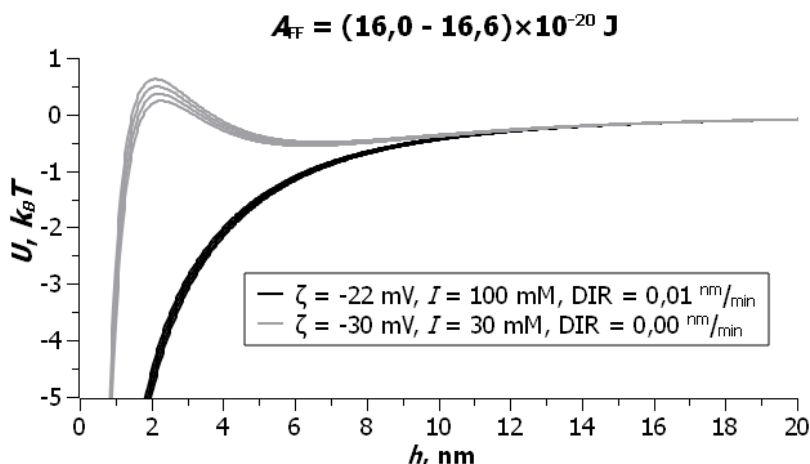

Figure 7 – Hypothetical Hamaker diagrams based on molecular attraction, A_{FF} = (16.0 to 16.6)$\times 10^{-20}$ J, and electrostatic repulsion.

Therefore, the experimental CCC is ca. one order of magnitude higher than the predicted threshold calculated with the A_{FF} values estimated in organic solvents. As it was mentioned above, an interaction that stabilizes the hydrosol should be expected. According to Derjaguin and Churaev, a structural (hydration) contribution to the disjoining pressure must be taken into account [26]. In other words, the U

value in Eq. 1 may contain an additional quantity, U_s, Eq. (3).

$$U_s = Kl \exp(-h/l) . \qquad (3)$$

Here K and l are constants; for hydrophilic and hydrophobic surfaces, $K > 0$ (structural repulsion) and $K < 0$ (structural attraction), respectively. Without knowing the two constants, K and l, it is difficult to draw precise

quantitative conclusions. In fact, the additional contribution, U_s , is opposed to the second item of the rhs of Eq. 1, but the type of the function is exponential. Approximate estimation for A_{FF} = 7.0×10^{-20} J is as follows: at 30 mM NaCl and ς = –30 mV, the U_{max} value is 26 k_BT. This value is much higher than that given in Figure 7. If the U value is compared at the distance, which corresponds to the barrier maximum in Figure 7, the difference is around 13 k_BT. In any case, the model proposed in the present paper looks out as self-consisted. This also is in line with numerous reports devoted to specific fullerene–water interactions [2, 10, 27–31].

CONCLUSIONS. The C$_{70}$ hydrosol prepared by solvent-exchange method (a system of the son/nC$_{70}$ type) is characterized by a electrokinetic potential of –40 ± 4 mV and particle size 97±3 nm at fullerene concentration of 3.3×10^{-6} M. The critical concentrations of coagulation (CCC) values are decreasing from 250 to 130 mM NaCl along with the rise of the hydrosol concentration from 3.3×10^{-6} to 6.9×10^{-5} M. The CCC for the CTAB surfactant is about 5×10^{-3} mM, i.e., fifty thousand times lower. Higher CTAB concentrations lead to overcharging of the colloidal particles up to ζ = + 40 mV and stabilization of the hydrosol.

Using the DLVO theory to explain the coagulation of the hydrosol by NaCl allows determining the Hamaker constant of the C$_{70}$–C$_{70}$ interaction in vacuum, if only electrostatic repulsion and molecular attraction are taking into account: $A_{FF} \approx 7×10^{-20}$ J. On the other hand, if the value A_{FF} = (16.0–16.6)×10^{-20} J, obtained earlier during the study of organosols, is used, then the data for hydrosols can be explained only by taking into account an additional type of interactions. Following the

terms of Churaev and Derjaguin, one should take into account the structural contribution to the interaction energy, U_s , which stabilizes the hydrosol.

ГІДРОЗОЛЬ ФУЛЕРЕНУ C$_{70}$: СИНТЕЗ ТА СТАБІЛЬНІСТЬ В ЕЛЕКТРОЛІТИЧНИХ РОЗЧИНАХ

М. О. Марфунін,[1] В. К. Клочков,[2] П. М. Радіонов,[1] М. О. Мчедлов-Петросян[1]

[1]*Харківський національний університет імені В. Н. Каразіна, пл. Свободи, 4, Харків 61022, Україна*
[2]*Інститут сцинтиляційних матеріалів НАН України, Харків 61001, Україна*
e-mail: mchedlov@karazin.ua

Статтю присвячено синтезу та характеризації гідрозолю C$_{70}$ і його коагуляції хлоридом натрію та бромідом цетилтриметиламонію (CTAB). При концентрації C$_{70}$ 3.3×10^{-6} M електрокінетичний потенціал дорівнює ζ = –40 ± 4 мВ, а розмір колоїдних частинок, виражений як Zeta-average,

дорівнює 97±3 нм; при концентраціях C_{70} 1.7×10^{-5} і 6.9×10^{-5} M розмір частинок залишається таким же: 99–100 нм. Значення критичної концентрації коагуляції (ССС) було визначено, використовуючи залежність швидкості зростання діаметру від концентрації NaCl. Значення ССС залежать від концентрації гідрозолю: вони дорівнюють 250, 145 і 130 мМ при концентраціях C_{70} 3.3×10^{-6}, 1.7×10^{-5} і 6.9×10^{-5} M, відповідно. Значення ССС при коагуляції за допомогою ЦТАБ є набагато нижчим: $\approx 5\times10^{-3}$ мМ. Але при концентрації ЦТАБ 0.02 мМ спостерігаємо перезарядження до $\zeta = +40$ мВ і стабілізацію колоїдних частинок. Інтерпретація коагуляції гідрозолю хлоридом натрію за допомогою теорії ДЛФО робить можливим оцінку константи Гамакера для взаємодії C_{70}–C_{70} у вакуумі, $A_{FF} \approx 7\times10^{-20}$ Дж, якщо враховувати тільки електростатичне відштовхування та молекулярне притягання. З іншого боку, якщо використовувати значення $A_{FF} = (16.0–16.6)\times10^{-20}$ J, знайдене раніше при вивченні органозолів, тоді результат для гідрозолю стає можливим тільки при введенні до розгляду додаткового типу взаємодій. Згідно з Чураєвим і Дерягіним, треба враховувати внесок структурної складової до загальної енергії взаємодії, який стабілізує гідрозоль.

Keywords: гідрозоль фулерену C_{70}, електрокінетичний потенціал, хлорид натрію, бромід цетилтриметиламонію, критична концентрація коагуляції, теорія Дерягіна – Ландау – Вервея – Овербека, діаграма Гамакера, константа Гамакера фулерен – фулерен, структурний внесок у взаємодію між частинками.

REFERENCES

1. Kyzyma O. A. Liquid systems with fullerenes in organic solvents and aqueous media. *Ukrainian J. Phys.* 2020. **65** (9): 761–767. https://doi.org/10.15407/ujpe65.9.761

2. Mchedlov-Petrossyan N.O. Fullerenes in aqueous media: A review. *Theoretical and Experimental Chemistry*. 2020. **55** (6): 361–391. https://doi.org/10.1007/s11237-020-09630-w

3. Kharissova O. V., Oliva González C. M., Kharisov B.L. Solubilization and Dispersion of Carbon Allotropes in Water and Non-Aqueous Solvents. *Industrial & Engineering Chemistry Research.* 2018. **57** (38): 12624–12645. https://doi.org/10.1021/acs.iecr.8b02593

4. Mikheev I. V., Sozarukova M. M., Izmailov D. Yu., Kareev I. E., Proskurnina E. V., Proskurnin M. A. Antioxidant Potential of Aqueous Dispersions of Fullerenes C_{60}, C_{70}, and Gd@C_{82}. *International Journal of Molecular Sciences* 2021. **22** (5838): 1–13. https://doi.org/10.3390/ijms22115838

5. Mikheev I. V., Pirogova M. O., Usoltseva L. O., Uzhel A. S., Bolotnik T. A., Kareev I. E., Bubnov V. P., Lukonina N. S., Volkov D. S., Goryunkov A. A., Korobov M. V., Proskurnin M. A. Green and rapid preparation of long-term stable aqueous dispersions of fullerenes and endohedral fullerenes: The pros and cons of an ultrasonic probe. *Ultrasonics Sonochemistry.* 2021. **73**: 105533. https://doi.org/10.1016/j.ultsonch.2021.105533

6. Damasceno J. P. V., Hof F., Chauvet O., Zarbin A. J. G., Pénicaud A. The role of functionalization on the colloidal stability of aqueous fullerene C_{60} dispersions prepared with fullerides. *Carbon.* 2021. **173**: 1041–1047. https://doi.org/10.1016/j.carbon.2020.11.082

7. Wei X., Wu M., Qi L., Xu Z., Selective solution-phase generation and oxidation reaction of C_{60}^{n-} (n = 1,2) and formation of an aqueous colloidal solution of C_{60}. *J. Journal of the Chemical Society, Perkin Transactions 2.* 1997. 1389–1394. https://doi.org/10.1039/a607336k

8. Noneman K., Muhich C., Ausman K., Henry M., Jankowski E. Molecular simulations for understanding the stabilization of fullerenes in water. *Journal of Computational Science Education*. 2021. **12** (1): 39–48
https://doi.org/10.22369/issn.2153-4136/12/1/6

9. Murdianti B. S., Damron J. T., Hilburn M. E., Maples R. D., HikkaduwaKoralege R. S., Kuriyavar S. I., Ausman K. D. C$_{60}$ Oxide as a Key Component of Aqueous C$_{60}$ Colloidal Suspensions. *Environmental Science & Technology*. 2012. **46:** 7446–7453.
https://dx.doi.org/10.1021/es2036652

10. Mchedlov-Petrossyan N. O., Marfunin M. O. Formation, Stability, and Coagulation of Fullerene Organosols: C$_{70}$ in Acetonitrile–Toluene Solutions and Related Systems. *Langmuir*. 2021. **37** (23): 7156–7166.
https://doi.org/10.1021/acs.langmuir.1c00722.

11. Mchedlov-Petrossyan N. O., Al-Shuuchi Y. T. M., Kamneva N. N., Marynin A. I. , Klochkov V. K. The Interactions of the Nanosized Aggregates of Fullerene C$_{60}$ with Electrolytes in Methanol: Coagulation and Overcharging of Particles. *Langmuir*. 2016. **32** (39): 10065–10072.
http://dx.doi.org/10.1021/acs.langmuir.6b02533

12. Mchedlov-Petrossyan N. O., Kamneva N. N., Al-Shuuchi Y. T .M., Marynin A. I. Interaction of C$_{60}$ aggregates with electrolytes in acetonitrile. *Colloids and Surfaces A: Physicochemical and Engineering Aspects*. 2017. **516**: 345–353.
http://dx.doi.org/10.1016/j.colsurfa.2016.12.035

13. Chen K. L., Elimelech M. Aggregation and deposition kinetics of fullerene (C$_{60}$) nanoparticles. *Langmuir.* 2006. **22** (26): 10994–11001.
https://doi.org/10.1021/la062072v

14. Chen K. L., Elimelech M. Relating colloidal stability of fullerene (C$_{60}$) nanoparticles to nanoparticle charge and electrokinetic properties. *Environmental Science & Technology*. 2009. **43** (19): 7270–7276.
https://doi.org/10.1021/es900185p

15. Meng Z., Hashmi S. M., Elimelech M. Aggregation rate and fractal dimension of fullerene nanoparticles via simultaneous multiangle static and dynamic light scattering measurement. *Journal of Colloid and Interface Science.* 2013. **392**: 27–33.
https://doi.org/10.1016/j.jcis.2012.09.088

16. Aich N., Flora J. R. V., Saleh N. B. Preparation and characterization of stable aqueous higher-order fullerenes. *Nanotechnol.* 2012. **23** (055705): 1–9.
http://doi.org/10.1088/0957-4484/23/5/055705

17. Aich N., Boateng L. K., Sabaraya I. V. Das D., Flora J. R. V., Saleh N. B. Aggregation Kinetics of Higher-Order Fullerene Clusters in Aquatic Systems. *Environmental Science & Technology*. 2016. **50** (7): 3562–3571.
https://doi.org/10.1021/acs.est.5b05447

18. Mikheev I. V., Bolotnik T. A., Volkov D. S., Korobov M.V., Proskurnin M. A. Approaches to the determination of C$_{60}$ and C$_{70}$ fullerene and their mixtures in aqueous and organic solutions. *Nanosystems: Physics, Chemistry, Mathematics.* 2016. **7** (1): 104–110. https://doi.org/10.17586/2220-8054-2016-7-1-104-110

19. Delgado A. V., González-Caballero F., Hunter R. J., Koopal L. K., Lyklema J. Measurement and interpretation of electrokinetic phenomena. *Journal of Colloid and Interface Science* 2007. **309**: 194–224
https:/doi.org/10.1016/j.jcis.2006.12.075

20. Ohshima H. A simple expression for Henry's function for the retardation effect in electrophoresis of spherical colloidal particles. *Journal of Colloid and Interface Science* 1994. **168**: 269–271. https://doi.org/10.1006/jcis.1994.1419

21. Михеев И. В. Дисс. … канд. хим. наук. Москва: МГУ, 2018.

22. Mchedlov-Petrossyan N. O., Klochkov V. K., Andrievsky G. V. Colloidal dispersions of fullerene C$_{60}$ in water: some properties and regularities of coagulation by electrolytes. *Journal of the Chemical Society, Faraday Transactions*. 1997. **93** (24): 4343–4346.
https://doi.org/10.1039/A705494G

23. Wang W., Gu B., Liang L., Hamilton W.B.

Adsorption and Structural Arrangement of Cetyltrimethylammonium Cations at the Silica Nanoparticle–Water Interface. *Journal of Physical Chemistry B*. 2004. **108** (45): 17477–17483. https://doi/10.1021/jp048325f

24. Gigault, J., Budzinski, H. Selection of An Appropriate Aqueous Nano-Fullerene (nC_{60}) Preparation Protocol for Studying its Environmental Fate and Behavior, *Trends In Analytical Chemistry*. 2016. **80**: 1–11. https://doi.org/10.1016/j.trac.2016.02.019

25. Dukhin S. S.; Derjaguin B. V.; Semenikhin N. M. The interaction of two identical spherical colloidal particles in large distances (in Russian). *Doklady AN USSR*. 1970. **192**: 357–360.

26. Churaev N. V., Derjaguin B.V., Inclusion of structural forces in the theory of stability of colloids and films. *Journal of Colloid and Interface Science*. 1985. **103**: 542–553. https://doi.org/10.1016/0021-9797(85)90129-8

27. Brant J. A., Labille J., Bottero J.-Y., Wiesner M. R. Characterizing the impact of preparation method on fullerene cluster structure and chemistry. *Langmuir*. 2006. **22**: 3878–3885. https://doi.org/10.1021/la053293o

28. Ma X., Wiginton B., Bouchard D. Fullerene C_{60}: Surface energy and interfacial interactions in aqueous systems. *Langmuir*. 2010. **26**: 11886–11893. https://doi.org/10.1021/la101109h

29. Choi J. I., Snow S. D., Kim J.-H., Jang S. S., Interaction of C_{60} with water: first-principles modeling and environmental implications. *Environ. Sci. Technol*. 2015. **49**: 1529–1536. https://doi.org/10.1021/es504614u

30. Li L., Bedrov D., Smith G. D., A molecular-dynamics simulation study of solvent-induced repulsion between C_{60} fullerenes in water. *J. Chem. Phys*. 2005. **123**: No. 204504. https://doi.org/10.1063/1.2121647

31. Bedrov D., Smith G. D., Davande H., Li L. Passive transport of C_{60} fullerenes throuhj a lipid membrane: A molecula dynamics simulation study. *J. Phys. Chem. B* 2008. **112:** 2078–2084. https://doi.org/10.1021/jp075149c